

# Shortening of Cardiac Action Potential Duration Near an Insulating Boundary

John W. Cain<sup>1</sup> and David G. Schaeffer<sup>2</sup>

<sup>1</sup>Department of Mathematics and Center for the Study of Biological Complexity,  
1001 West Main Street, Virginia Commonwealth University, Richmond, VA 23284-2014 USA

<sup>2</sup> Department of Mathematics and Center for Nonlinear and Complex Systems,  
Duke University, Box 90320, Durham, NC 27708-0320 USA

January 3, 2008

## ABSTRACT

It is known, from both experiments and simulations, that cardiac action potentials are shortened near a nonconducting boundary. In the present paper, this effect is studied in a simple, two-current ionic model, with propagation restricted to a one-dimensional fiber. An asymptotic approximation for the dependence of action potential duration on distance to the boundary is derived. This estimate agrees well with simulations.

*Keywords:* action potential duration; insulating boundary; one-dimensional cable.

## 1 Introduction

Cardiac cells are *excitable* in the sense that a brief electrical stimulus can cause the transmembrane voltage  $v$  to experience a prolonged elevation known as an *action potential*. Action potentials propagate through tissue because neighboring cells are connected electrically via intercellular channels (called gap junctions). These propagating electrical waves coordinate the contraction of cardiac muscle as needed for effective pumping of blood. Understanding the timing of these waves is a first step towards detecting and preventing potentially fatal arrhythmias.

As usual, let us define the *action potential duration (APD)* as the amount of time in which the voltage remains elevated above a specified threshold  $v_{\text{thr}}$ . In experiments, the threshold voltage is chosen anywhere from 70 to 90 percent<sup>1</sup> recovery from the peak voltage to the resting voltage.

---

<sup>1</sup>In this study, our results are not especially sensitive to the choice of  $v_{\text{thr}}$ .

In recent *in vitro* experiments [4], a small piece of frog heart tissue was stimulated using a unipolar pacing electrode and APD was measured on the surface of the tissue with voltage-sensitive fluorescent dyes. Figure 1 shows the APD's measured along a representative radial line emerging from the stimulus site. The line terminates where the piece of tissue was cut from the whole heart. (Below we model this boundary with a Neumann condition.) As the figure shows, APD values near the electrode were 10% larger than values at the edge of the tissue. To prove that this effect was not simply the result of tissue inhomogeneity, the stimulating electrode was placed at several different sites around the tissue; always APD exhibited the same shortening with increasing distance from the electrode.

Although it is not apparent from an experiment in such a small sample, we believe that this dependence of APD on distance from the stimulus site is a boundary effect. We support this claim with simulations using the two-current ionic model of [8, 10], which will be described in Section 2. In the simulations shown in Figure 2a, on a cable 1 cm long, APD decreases approximately linearly with distance from the stimulus site. By contrast, in those of Figure 2b, on a cable 4 cm long, APD is independent of position away from the ends of the cable, is elevated locally near the stimulus end, and is depressed locally near the distal end. On a longer cable, the central region is wider but the elevation and depression near the ends are virtually unchanged<sup>2</sup>.

In this paper we study how the duration of a single action potential propagating along a long fiber<sup>3</sup> is changed near the end of the fiber. In order to avoid modeling the details of stimulation, we restrict our attention to the distal end of the fiber. Specifically, for the two-current model, we derive an asymptotic approximation for  $\delta APD(x)$ , the change in APD expressed as a function of distance  $x$  along the fiber from a non-conducting boundary. This analytical result for a simplified model sheds light on phenomena in more realistic models or experiments.

Although this shortening is a relatively small fraction of the total APD, such boundary effects may play a role in generating arrhythmias. For example, under rapid periodic pacing, tissue may bifurcate into a period-2 orbit called *alternans*: i.e., the response to identically spaced stimuli alternates between short and long APD's. In both simulations and experiments, as the pacing rate increases, alternans have been observed first and are strongest close to a boundary [7, 12].

The remainder of the paper is organized as follows. In Section 2, we recall the two-current ionic model [8, 10], including asymptotic estimates for APD in this model and the description of traveling waves in it. In Section 3, we derive our main result: an approximate formula for  $\delta APD(x)$  near an insulating boundary. Finally, in Section 4 we show that our approximation agrees well with simulations, and we characterize how this phenomenon depends on the parameters in the model.

---

<sup>2</sup>Other simulations have observed the same effect; see, for example, Section IV of Echebarria and Karma [6].

<sup>3</sup>In adopting a one-dimensional model we are neglecting how the curvature of the wave front might influence the voltage

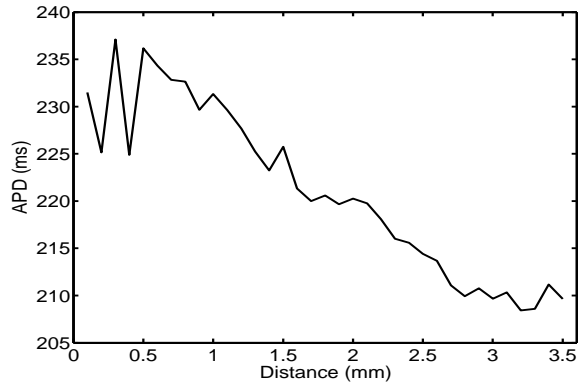


Figure 1: Experimentally measured spatial variation of APD. Stimuli were applied at  $x = 0$ , where  $x$  denotes distance from the pacing electrode.

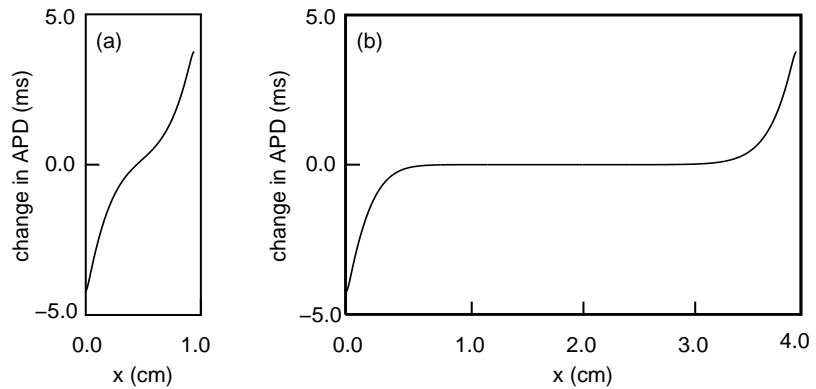


Figure 2: Spatial variation of APD in (a) a 1.0-cm cable and (b) a 4.0-cm cable as generated by numerical simulation of (4–5) with parameters from Table 1. Stimuli were applied at the *right* end of the fiber. The indicated variations are added to an unperturbed APD of 439.3 ms.

## 2 The two-current model

### 2.1 The equations

The two-current model [8, 10] for a patch<sup>4</sup> of tissue consists of two ordinary differential equations (ODEs) for two variables: the transmembrane voltage  $v(t)$  and an inactivation gate variable  $h(t)$ , both of which are dimensionless and scaled to vary between 0 and 1. The voltage equation takes the form

$$\frac{dv}{dt} = F(v, h) = J_{\text{in}}(v, h) + J_{\text{out}}(v), \quad (1)$$

where  $F(v, h)$  is a sum of inward and outward currents given by

$$J_{\text{in}}(v, h) = \frac{h}{\tau_{\text{in}}} v^2 (1 - v), \quad J_{\text{out}}(v) = -\frac{v}{\tau_{\text{out}}}. \quad (2)$$

The parameters  $\tau_{\text{in}}$  and  $\tau_{\text{out}}$  are time constants that specify the strength of the inward and outward currents, respectively. The other variable, the gate that regulates inward current flow, obeys the ODE

$$\frac{dh}{dt} = G(v, h) = \begin{cases} (1 - h)/\tau_{\text{open}}, & v < v_{\text{crit}} \\ -h/\tau_{\text{close}}, & v > v_{\text{crit}}. \end{cases} \quad (3)$$

Representative values for the time constants in (2,3) are given in Table 1.

Equations (1, 3) are easily modified to model the propagation of action potentials in a homogeneous one-dimensional cable—that is, an idealized fiber of cells electrically coupled via gap junctions. If  $x$  denotes distance along the fiber, the voltage  $v = v(x, t)$  obeys a partial differential equation (PDE)

$$\frac{\partial v}{\partial t} = \kappa \frac{\partial^2 v}{\partial x^2} + F(v, h), \quad (4)$$

where  $\kappa$  is a diffusion constant; and the gate variable satisfies

$$\frac{\partial h}{\partial t} = G(v, h), \quad (5)$$

which by contrast contains no  $x$ -derivatives. In a finite-length or semi-infinite cable, Neumann boundary conditions on the voltage, corresponding to no axial current, are imposed at the ends of the cable.

---

near the edges. This paper shows that one-dimensional effects are sufficient to explain the phenomenon.

<sup>4</sup>That is, a piece of tissue so small that spatial extent is negligible.

Parameter	Meaning	Units	Value
$\tau_{\text{in}}$	time constant	ms	0.2
$\tau_{\text{out}}$	time constant	ms	10
$\tau_{\text{open}}$	time constant	ms	130
$\tau_{\text{close}}$	time constant	ms	150
$v_{\text{crit}}$	critical voltage	dim'less	0.13
$\kappa$	diffusion constant	$\text{cm}^2/\text{ms}$	0.001

Table 1: Sample parameter values for the two-current model.

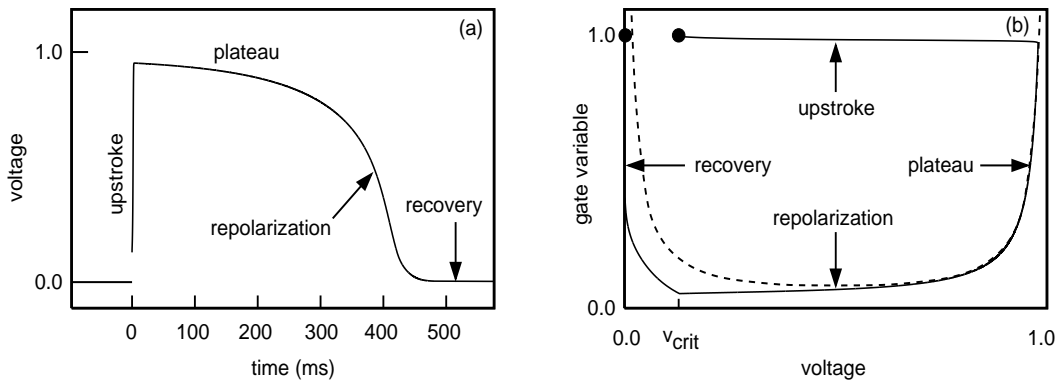


Figure 3: (a) Voltage trace illustrating the four phases of the action potential. (b) The corresponding phase plane trajectory. The dashed curve is the graph of the nullcline (8). Both trajectories were generated by numerical solution of (1–3) using the parameters in Table 1 and  $v(0) = 0.13$ ,  $h(0) = 1.0$ .

When numerical simulations are required, we will use the parameter values listed in Table 1. Note that these time constants satisfy

$$\tau_{\text{out}} \ll \tau_{\text{open}}, \tau_{\text{close}}. \quad (6)$$

Below we shall always assume the time scales are well-separated in this way, and we shall make asymptotic approximations based on the small parameter

$$\varepsilon = \frac{\tau_{\text{out}}}{\tau_{\text{close}}}. \quad (7)$$

## 2.2 Asymptotic estimates for APD in a patch

Observe that  $(v, h) = (0, 1)$  is a stable equilibrium of the ODEs (1,3). These equations exhibit excitability in that, if a stimulus raises the voltage slightly above this equilibrium value,

then the voltage increases further and remains elevated for a long period before returning to equilibrium, as sketched in Figure 3. The structure of such an action potential may be characterized with asymptotics using the fact that, because of (6), the voltage evolves much more rapidly than the gate unless  $(v, h)$  lies close to the nullcline  $\{dv/dt = 0\}$ . By (1,2), on this nullcline either  $v = 0$  or

$$h = \frac{\tau_{\text{in}}}{\tau_{\text{out}}} \frac{1}{v(1-v)}. \quad (8)$$

Alternatively, solving (8) for  $v$ , we obtain

$$v = v_{\pm}(h) = \frac{1}{2} \left( 1 \pm \sqrt{1 - \frac{h_{\text{min}}}{h}} \right), \quad (9)$$

where

$$h_{\text{min}} = \frac{4\tau_{\text{in}}}{\tau_{\text{out}}}. \quad (10)$$

Phase	Name	Duration (order of mag.)	Simplification	Dominant equation
1	Upstroke	$\tau_{\text{in}}$	$h \approx \text{Const}$	(1)
2	Plateau	$\tau_{\text{close}}$	$J_{\text{in}} + J_{\text{out}} \approx 0$	(3)
3	Repolarization	$\tau_{\text{close}}^{1/3} \tau_{\text{out}}^{2/3}$	$h \approx \text{Const}$	(1)
4	Recovery	$\tau_{\text{open}}$	$v \approx 0$	(3)

Table 2: Summary of asymptotics during the four phases of an action potential

As illustrated in Figure 3, an action potential has four distinct phases. The dominant behavior in each phase may be described as follows and as summarized in Table 2. (See [10] for a more detailed discussion of the asymptotics.)

1. *Upstroke phase*: Following a successful stimulus, the strong inward current  $J_{\text{in}}$  raises the voltage until it reaches  $V_+ = v_+(1)$  on the right branch of the nullcline (9). This occurs in a time on the order of  $\mathcal{O}(\tau_{\text{in}})$ .
2. *Plateau phase*: As the gate closes according to (3)—i.e.,  $h(t) = \exp(-t/\tau_{\text{close}})$ —the voltage follows the nullcline (9), keeping the inward and outward currents balanced.
3. *Repolarization phase*: When the gating variable reaches  $h_{\text{min}}$  given by (10), the solution “falls off the nullcline”. I.e., at this point the inward current is no longer able to balance the outward current, and the voltage drops toward zero in a time that is short<sup>5</sup> compared to  $\tau_{\text{close}}$ .

---

<sup>5</sup>As asserted in equation (12) below, the duration of this phase is  $\mathcal{O}(\tau_{\text{close}}^{1/3} \tau_{\text{out}}^{2/3})$ .

4. *Recovery phase, or diastole:* The voltage stays small and the gate reopens with a time constant  $\tau_{\text{open}}$ .

In Section 4.2 it will be useful to have estimates for the duration of such an action potential, which we denote by  $\text{APD}_{\text{max}}$  since this action potential is the largest possible APD that a cell can exhibit<sup>6</sup>. An APD consists of all of phase 2 plus parts of phases 1 and 3. According to (6), phases 1 and 3 are much shorter than phase 2. In fact, in leading-order asymptotics,  $\text{APD}_{\text{max}}$  equals the time in phase 2 during which, starting from 1, the gate decays exponentially to  $h_{\text{min}}$ . Thus,

$$\text{APD}_{\text{max}} \sim \tau_{\text{close}} \ln \left( \frac{1}{h_{\text{min}}} \right). \quad (11)$$

Strictly speaking, to compute APD we should introduce a threshold voltage  $v_{\text{thr}}$  and define APD as the length of time that  $v(t) > v_{\text{thr}}$ . However, because the voltage evolves rapidly in phases 1 and 3, the low-order estimates for  $\text{APD}_{\text{max}}$  do not depend on  $v_{\text{thr}}$ . Nevertheless, the choice of  $v_{\text{thr}}$  does affect (slightly) the boundary corrections to APD computed in Section 3.

At the next order of asymptotics, phase 3 *does* contribute to  $\text{APD}_{\text{max}}$ . At first glance, one might guess that the duration of phase 3 is  $\mathcal{O}(\tau_{\text{out}})$  since this parameter characterizes the strength of  $J_{\text{out}}$ , the dominant current in this phase; this would represent an  $\mathcal{O}(\varepsilon)$  correction to (11), where  $\varepsilon$  is given by (7). However, at the start of phase 3, pending further decay of  $h$  and hence of  $J_{\text{in}}$ , the two currents nearly cancel one another. As shown in [2], this effect slows the decrease of the voltage and thus lengthens the APD. (Cf. The analysis of Cartwright [3] and Dorodnicyn [5] concerning relaxation oscillations in the van der Pol equation.) Specifically, we find that (11) is augmented to

$$\text{APD}_{\text{max}} \sim \tau_{\text{close}} \left\{ \ln \left( \frac{1}{h_{\text{min}}} \right) + z_1 \varepsilon^{2/3} \right\}, \quad (12)$$

where  $z_1 = 2.33811\dots$  is the first zero of the Airy function,  $\text{Ai}(-z)$ . This formula predicts  $\text{APD}_{\text{max}}$  with surprisingly high accuracy. For example, using the parameters in Table 1, we estimate from formula (12) that  $\text{APD}_{\text{max}} = 436.5$  ms, less than 1% below the true value (obtained numerically) of 439.3 ms. By comparison, the leading-order estimate (11) predicts that  $\text{APD}_{\text{max}} = 378.7$  ms, a relative error of 14%.

### 2.3 Traveling-wave solutions in an infinite fiber

We seek a traveling-wave solution of equations (4, 5),

$$v(x, t) = V(t + x/c), \quad h(x, t) = H(t + x/c), \quad (13)$$

---

<sup>6</sup> $\text{APD}_{\text{max}}$  refers to an action potential produced by a stimulus following a long diastolic interval. Under periodic pacing, shorter action potentials are produced, especially under rapid pacing (which is not considered here).

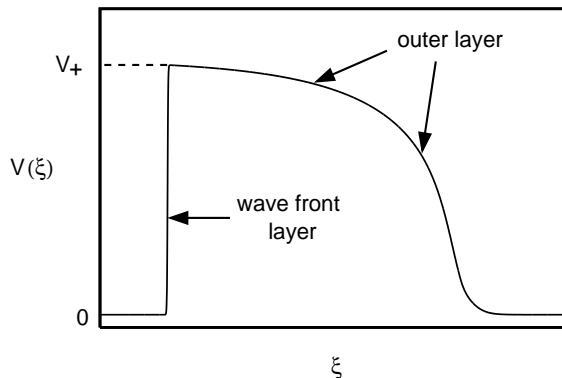


Figure 4: Voltage profile of a traveling pulse moving from right to left on an infinite cable.

where the speed  $c$  is to be determined. This yields a system of two ODEs for  $V$  and  $H$  with independent variable  $\xi = t + x/c$ . It is shown in [1] that, if  $\tau_{\text{in}}/\tau_{\text{out}} < 4/25$ , then for sufficiently small  $\varepsilon$ , this system indeed admits a traveling-wave solution<sup>7</sup>. For  $\xi < 0$  the solution is quiescent ( $V \equiv 0, H \equiv 1$ ); for  $\xi > 0$  it is well-approximated by phases 2,3, and 4 of an action potential in a patch model; and these two outer regions are separated by an inner or wave-front layer in which voltage diffusion is crucial (see Figure 4).

In the inner layer, in a time that is  $\mathcal{O}(\tau_{\text{in}})$ , the voltage climbs from 0 to  $V_+$ , where (cf. (9))

$$V_{\pm} = v_{\pm}(1) = \frac{1}{2} \left( 1 \pm \sqrt{1 - h_{\text{min}}} \right). \quad (14)$$

We may approximate  $H \equiv 1$  in the wave-front layer because, by equation (6), the time constants regulating  $H$  are much larger than  $\tau_{\text{in}}$ . In terms of a scaled inner coordinate  $\tilde{\xi} = \tau_{\text{in}}^{-1}(t + x/c)$ , to leading order the inner solution solves

$$V' = \frac{1}{c^2} \frac{\kappa}{\tau_{\text{in}}} V'' + \tau_{\text{in}} F(V, 1), \quad (15)$$

where prime indicates differentiation with respect to  $\tilde{\xi}$ . Equation (15) is subject to boundary conditions

$$\lim_{\tilde{\xi} \rightarrow -\infty} V(\tilde{\xi}) = 0, \quad \lim_{\tilde{\xi} \rightarrow \infty} V(\tilde{\xi}) = V_+. \quad (16)$$

<sup>7</sup>If  $4/25 < \tau_{\text{in}}/\tau_{\text{out}} < 1/4$ , equations (4,5) still admit a traveling-wave solution but with slightly different structure. Specifically, similar to the FitzHugh-Nagumo model, the gate  $h$  does not decay all the way to  $h_{\text{min}}$  but only to a value in  $(h_{\text{min}}, 1)$  that is determined by matching speeds of the leading and trailing edges of the wave. We assume that  $\tau_{\text{in}}/\tau_{\text{out}} < 4/25$  since in the physiologically interesting cases this parameter is small. For example,  $\tau_{\text{in}}/\tau_{\text{out}} = 0.02$  for the parameters in Table 1.

**Proposition 2.1.** *Problem (15,16) has a solution if*

$$c = \left( \frac{1}{2}V_+ - V_- \right) \sqrt{\frac{2\kappa}{\tau_{\text{in}}}}. \quad (17)$$

*Proof.* See Zeldovich et al. [15] or, for a more modern approach, Murray [11].  $\square$

Incidentally, using the parameter values in Table 1, (17) predicts  $c = 46.9$  cm/sec, while we find  $c = 46.7$  cm/sec from numerical solution of (4,5). This good agreement provides *a posteriori* justification for the approximation that  $H$  is constant in the inner layer.

In the outer region  $\xi > 0$ , provided  $\tau_{\text{in}}/\tau_{\text{out}} < 4/25$ , the traveling-wave solution of (4,5) solves the ODE

$$\frac{dV}{d\xi} = F(V, H) \quad \frac{dH}{d\xi} = G(V, H),$$

subject to initial conditions

$$V(0) = V_+ \quad H(0) = 1. \quad (18)$$

This solution, which matches continuously onto the inner solution, corresponds to phases 2, 3, and 4 of an action potential in a patch.

While referring to [1] for proofs, let us offer a heuristic argument that this construction satisfies the PDE (4,5) to leading order. Consider for example values of  $\xi$  corresponding to phase 2 of an action potential. In this range of  $\xi$

$$\frac{dV}{d\xi} \sim \frac{1}{\tau_{\text{close}}}, \quad \frac{d^2V}{d\xi^2} \sim \frac{1}{\tau_{\text{close}}^2}.$$

Thus, substituting into (13) and recalling (17), we see that

$$\kappa \frac{\partial^2 v}{\partial x^2} \sim \frac{\tau_{\text{in}}}{\tau_{\text{close}}^2} \sim \frac{\tau_{\text{in}}}{\tau_{\text{close}}} \frac{\partial v}{\partial t}.$$

Hence, since  $\tau_{\text{in}}/\tau_{\text{close}} \ll 1$ , the diffusion term, which distinguishes the PDE (4) from the ODE (1), is of higher order. Similarly for phases 3 and 4.

We summarize: If  $\tau_{\text{in}}/\tau_{\text{out}} < 4/25$ , then to leading order, the traveling wave differs from an action potential on a patch only in the wave-front layer. In this layer, the speed of the traveling wave is determined by the balance between diffusion and the strength of the inward current.

### 3 A formula for the boundary correction to APD

#### 3.1 The governing equations on a half-line

Consider a solitary action potential propagating along a long, homogeneous fiber toward an insulating boundary at  $x = 0$ . Intuitively, the shortening of APD as it approaches the

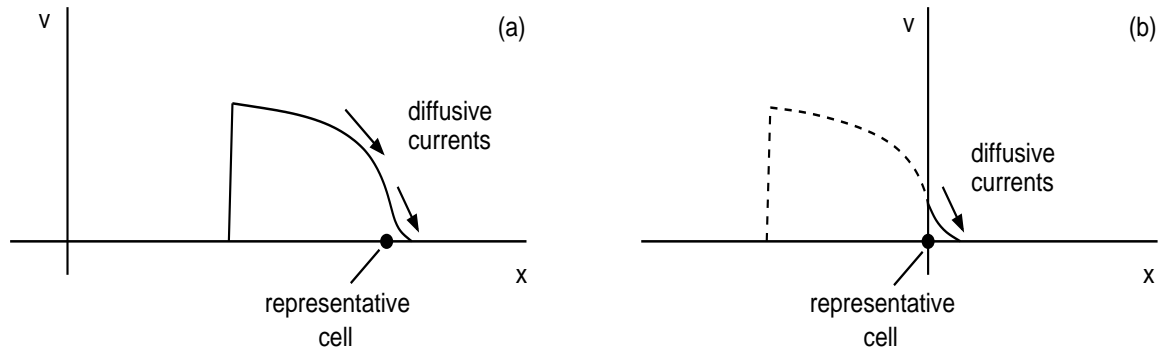


Figure 5: Diffusive currents for a pulse (a) far from an insulating boundary and (b) after reaching the insulating boundary.

boundary may be understood by comparing the diffusive currents near two representative cells, as shown in Figure 5, one far from the boundary and one at the boundary. For both cases, as the wave back passes through the cell, the diffusive current  $-\kappa\partial v/\partial x$  moves charge from this cell to its neighbors on the right, where the action potential has progressed further. Far from the boundary, as in Figure 5a, the loss of charge to neighbors on the right is approximately balanced by the gain of charge from neighbors on the left. By contrast, near the boundary, as in Figure 5b, neighbors on the left are missing. Thus, in the latter case the diffusive current lowers the voltage in the wave-back region and hence shortens the APD.

Mathematically, a propagating action potential can be modeled using (4, 5) on a half-space  $\{0 < x < \infty, -\infty < t < \infty\}$  subject to the boundary condition

$$\frac{\partial v}{\partial x}(0, t) = 0 \quad (-\infty < t < \infty) \quad (19)$$

and the initial conditions

$$\lim_{t \rightarrow -\infty} \max_{0 \leq x < \infty} |v(x, t) - V(t + x/c)| = 0 \quad (20)$$

$$\lim_{t \rightarrow -\infty} \max_{0 \leq x < \infty} |h(x, t) - H(t + x/c)| = 0. \quad (21)$$

In words, the initial conditions require that the difference between the exact solution and a pure traveling-wave solution is negligible when the pulse is far from the boundary.

We seek a solution of this problem of the form

$$v(x, t) = V(t + x/c) + w(x, t), \quad h(x, t) = H(t + x/c), \quad (22)$$

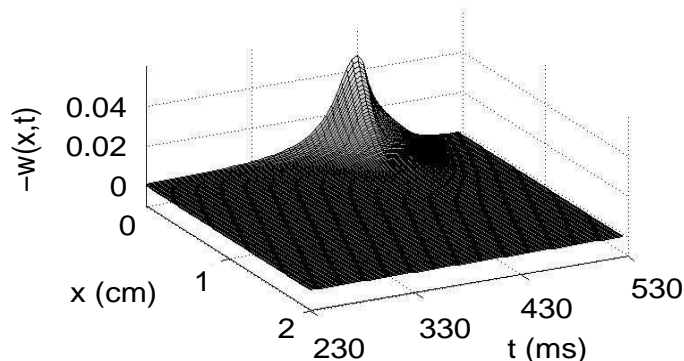


Figure 6: Plot of  $-w(x,t)$  versus  $x$  and  $t$  obtained by numerical solution of (4,5) using the parameters in Table 1. The maximum magnitude of  $w(x,t)$  is approximately 0.045, and is achieved at the insulating boundary  $x = 0$  as the wave back approaches.

where  $w$  is a correction to the voltage  $V$  in the traveling wave solution. (We neglect the correction to the gate variable, which is of higher order since the gate evolves more slowly than the voltage.) Since the maximum correction to APD at the boundary is hardly 1% (cf. Figure 2), one suspects  $w$  is a small correction. The computations summarized in Figure 6 verify this—the maximum value of  $w$  is approximately 0.045 while the voltage is of order unity<sup>8</sup>. Thus, substituting (22) into (4,19,20) and gathering the leading-order terms in  $w$ , we obtain the linearized problem

$$\frac{\partial w}{\partial t} = \kappa \frac{\partial^2 w}{\partial x^2} + \gamma(x,t)w \quad (x > 0, -\infty < t < \infty) \quad (23)$$

$$\frac{\partial w}{\partial x}(0,t) = -\frac{1}{c}V'(t) \quad (-\infty < t < \infty) \quad (24)$$

$$\lim_{t \rightarrow -\infty} w(\cdot, t) = 0, \quad (25)$$

where

$$\gamma(x,t) = \frac{H(t+x/c)}{\tau_{\text{in}}} [2V(t+x/c) - 3V^2(t+x/c)] - \frac{1}{\tau_{\text{out}}}. \quad (26)$$

In order to obtain an explicit solution, we shall solve (23–25) making the approximation  $\gamma(x,t) \approx \gamma(0,t)$ : i.e.,

$$\gamma(x,t) \approx \gamma(t) = \frac{H(t)}{\tau_{\text{in}}} [2V(t) - 3V^2(t)] - \frac{1}{\tau_{\text{out}}}. \quad (27)$$

<sup>8</sup>Further indirect evidence that  $w$  is small is supplied by the fact that our estimates based linearizing the equations with respect to  $w$  agree so well with numerical simulations—see Figure 7.

This approximation will be discussed in Section 4.3.

### 3.2 Solution of the linearized problem

As a first step in attacking (23–25), we solve an analogous problem for the heat equation. Specifically, consider

$$\frac{\partial w}{\partial t} = \kappa \frac{\partial^2 w}{\partial x^2} \quad (x > 0, \quad -\infty < t < \infty) \quad (28)$$

$$\kappa \frac{\partial w}{\partial x}(0, t) = -j(t) \quad (-\infty < t < \infty) \quad (29)$$

$$\lim_{t \rightarrow -\infty} w(x, t) = 0 \quad (x > 0) \quad (30)$$

where in (29) we assume that  $j$  is bounded and integrable. The minus sign in (29) reflects the fact that a net influx of heat corresponds to a negative temperature gradient. The solution of (28–30) is given by

$$w(x, t) = \int_0^\infty K(x, s) j(t - s) ds, \quad (31)$$

where

$$K(x, t) = \sqrt{\frac{1}{\pi \kappa t}} \exp\left(-\frac{x^2}{4\kappa t}\right). \quad (32)$$

One may derive (31) by (i) defining  $\tilde{w}(x, t) = w(x, t) - xj(t)$ , which satisfies a homogeneous Neumann boundary condition but an inhomogeneous equation [14], (ii) solving for  $\tilde{w}$  by making an even extension to the whole line, and (iii) manipulating the resulting solution, including an integration by parts.

If the coefficient  $\gamma$  in (23) depends only on  $t$ , then we may reduce this equation to the heat equation by introducing an integrating factor. Specifically, let

$$\Gamma(t) = \int_0^t \gamma(s) ds. \quad (33)$$

Then (23) may be rewritten as

$$\frac{\partial}{\partial t}[e^{-\Gamma(t)}w] = \kappa \frac{\partial^2}{\partial x^2}[e^{-\Gamma(t)}w].$$

Applying (31), we find that the solution of (23–25) is given by

$$w(x, t) = \frac{\kappa}{c} \int_0^\infty K(x, s) e^{\Gamma(t) - \Gamma(t-s)} V'(t - s) ds. \quad (34)$$

### 3.3 The boundary correction to APD

We apply formula (34) to extract the spatial variation in APD in the vicinity of the insulating boundary. Given  $x \geq 0$ , we wish to estimate the amount of time in which the voltage  $v(x, t)$  remains elevated above the threshold voltage  $v_{\text{thr}}$ . To do so, we must determine the two times  $t$  for which

$$v(x, t) = V\left(t + \frac{x}{c}\right) + w(x, t) = v_{\text{thr}} \quad (x \geq 0 \text{ fixed}); \quad (35)$$

i.e., the arrival times at  $x$  of the wave front and of the wave back.

In the asymptotic construction of the traveling wave in Section 2.3, the wave front of the unperturbed solitary pulse reaches the boundary  $\{x = 0\}$  at time  $t = 0$ ; and the wave back at  $t = \text{APD}_{\text{max}}$ . In other words,

$$V(0) = V(\text{APD}_{\text{max}}) = v_{\text{thr}}. \quad (36)$$

Using (36) to generate a first estimate, we seek approximate times when (35) is satisfied by assuming

$$t + x/c = \delta_1(x), \quad \text{or} \quad t + x/c = \text{APD}_{\text{max}} + \delta_2(x), \quad (37)$$

where  $\delta_i(x)$ , representing the effect of the perturbing term  $w$  in (35), is small. Expanding  $V$  about 0 or  $\text{APD}_{\text{max}}$ , invoking (36), and neglecting  $\delta_i(x)$  in the argument of  $w$ , we simplify (35) to

$$V'(0)\delta_1(x) + w(x, -x/c) = 0, \quad \text{or} \quad V'(\text{APD}_{\text{max}})\delta_2(x) + w(x, \text{APD}_{\text{max}} - x/c) = 0.$$

Solving these linear equations for  $\delta_i(x)$ , we compute that the *change* in APD due to pulse interaction with the boundary is given by

$$\delta \text{APD}(x) \equiv \delta_2(x) - \delta_1(x) \approx -\frac{w(x, \text{APD}_{\text{max}} - x/c)}{V'(\text{APD}_{\text{max}})} + \frac{w(x, -x/c)}{V'(0)}. \quad (38)$$

Since  $V'(0) = \mathcal{O}(\tau_{\text{in}}^{-1})$  represents the steep slope (see Figure 4) of the wavefront of the undisturbed traveling pulse, the second term in (38) makes only a higher-order contribution to  $\delta \text{APD}$ . Retaining only the first term in (38) and recalling (34), we find our main estimate

$$\delta \text{APD}(x) \approx -\frac{\kappa}{c} \int_0^\infty K(x, s) e^{\Gamma(\text{APD}_{\text{max}} - x/c) - \Gamma(\text{APD}_{\text{max}} - x/c - s)} \frac{V'(\text{APD}_{\text{max}} - x/c - s)}{V'(\text{APD}_{\text{max}})} ds. \quad (39)$$

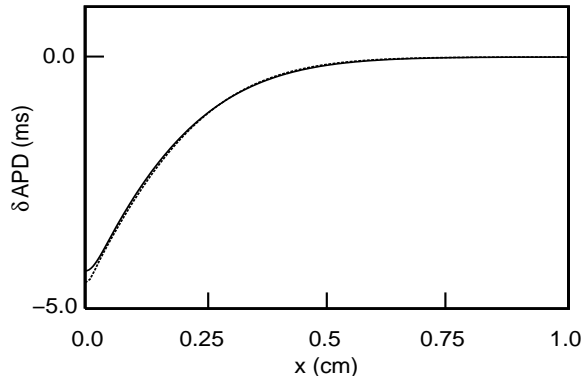


Figure 7: Comparison of  $\delta\text{APD}(x)$  as predicted by (39) (dashed curve) and by numerical solution of the original PDEs (solid curve).

## 4 Discussion and conclusions

### 4.1 Numerical simulations

Computer simulations show that the shortening of APD predicted by (39) is in good quantitative agreement with results from numerical solutions of (4–5). Specifically, Figure 7 shows a comparison of the actual change in APD (solid curve) with the change predicted by (39) (dashed curve). The solid curve was generated by numerical simulation of (4–5) using the parameter values in Table 1, a threshold voltage  $v_{\text{thr}} = v_{\text{crit}} = 0.13$ , and a cable length of 4 cm. Initially, the cable was at rest ( $v = 0$  and  $h = 1$  for all cells). Then, voltage was suddenly raised to  $v = 0.8$  for all cells with  $3.95 \leq x \leq 4.0$ , eliciting an action potential propagating from right to left. The plot shows  $\delta\text{APD}(x)$  in the region within 1 cm of the distal end of the cable. In generating the dashed curve using formula (39),  $\Gamma$  and  $V'$  were computed by numerical simulation of the traveling wave.

Incidentally, the small discrepancy between the two graphs in Figure 7 is due to the interaction of the wave *front* of the pulse with the boundary, which is neglected in (39): Near a boundary, the speed of an approaching pulse is accelerated because no diffusive current need be supplied to neighboring cells on the left, which slightly lengthens APD. This effect is similar to the interaction of the wave back with the boundary that shortens APD, but it is smaller and more localized.

### 4.2 The width of the boundary-correction layer

In this subsection we argue that the shortening of APD is concentrated in a layer of thickness

$$\Delta x \sim \varepsilon^{-1/6} \sqrt{\kappa \tau_{\text{out}}} \quad (40)$$

near the boundary. Note that  $\sqrt{\kappa\tau_{\text{out}}}$  is the length constant of the tissue [9, 13].

The integrand in (39) may be decomposed into three factors,

$$K(x, s), \quad e^{\Gamma(\text{APD}_{\text{max}}-x/c)-\Gamma(\text{APD}_{\text{max}}-x/c-s)}, \quad \text{and} \quad \frac{V'(\text{APD}_{\text{max}}-x/c-s)}{V'(\text{APD}_{\text{max}})}.$$

The first factor, given by (32), is exponentially small if  $s \ll x^2/\kappa$ . In other words, no significant error is made if one restricts the integration variable  $s$  to values bounded away from zero,  $s \geq \mathcal{O}(x^2/\kappa)$ . In the third factor, the numerator  $V'(t)$  is largest for times in the repolarization phase (see Figure 8(a)). According to (12), this phase has width approximately

$$W = \tau_{\text{close}} z_1 \varepsilon^{2/3}, \quad (41)$$

which suggests making an approximation in (39) in which  $s$  is restricted to values such that

$$x/c + s < W. \quad (42)$$

This approximation cannot be justified on the basis of the third factor alone—as Figure 8 indicates,  $V'(t)$  has a long tail extending to times well before the wave back region. However, we now show that the second factor in (39) decays rapidly for  $s$  in this range (see Figure 8(b)), and this justifies restricting  $s$  as in (42).

According to (33), the exponent in the second factor equals

$$\int_{\text{APD}_{\text{max}}-x/c-s}^{\text{APD}_{\text{max}}-x/c} \gamma(s') ds'$$

where  $\gamma$  is given by (27). Since  $H$  varies more slowly than  $V$ , let us consider, as a first step, an approximation of  $\gamma$  obtained by fixing the argument of  $H$  in (27) at a representative time  $t = t_*$ . We choose  $t_* = \tau_{\text{close}} \ln h_{\text{min}}^{-1}$ , the lowest order estimate for  $\text{APD}_{\text{max}}$ , because  $H(t_*) = h_{\text{min}}$ , which yields the simple approximation

$$\gamma_{\text{approx}} = \frac{h_{\text{min}}}{\tau_{\text{in}}} [2V - 3V^2] - \frac{1}{\tau_{\text{out}}} = \frac{1}{\tau_{\text{out}}} [8V - 12V^2 - 1]. \quad (43)$$

Figure 9 helps one understand the behavior of this approximation.

- As shown in Figure 9(a,c), the quadratic expression on the right in (43) vanishes when  $V$  passes through  $1/2$  and through  $1/6$ .
- As indicated in Figure 9(b),  $\gamma_{\text{approx}}(t_*)$  is negative. (This conclusion may also be extracted from the asymptotics of Section 2.2.)
- $\gamma_{\text{approx}}$  becomes more and more negative as  $t$  decreases from  $t_*$ .

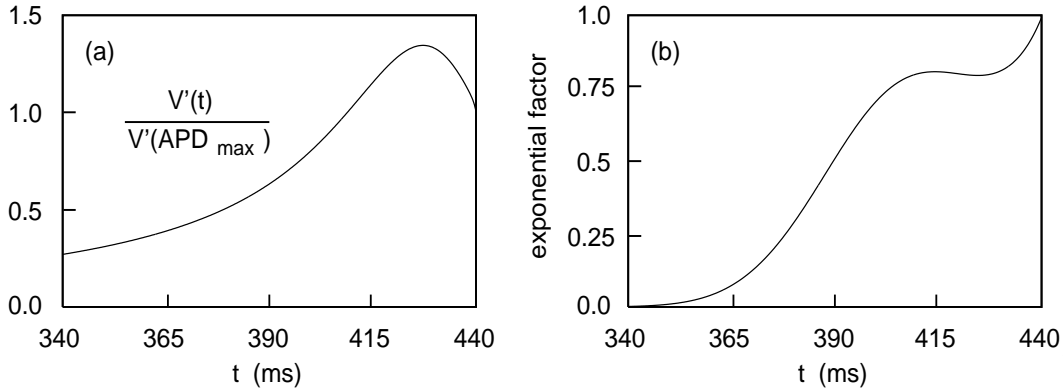


Figure 8: (a)  $V'(t)/V'(\text{APD}_{\max})$  versus  $t$ . (b) The exponential factor in the integrand of (39), with  $x = 0$ . Both graphs are terminated at  $t = \text{APD}_{\max}$ .

The exact  $\gamma$ , which is graphed in Figure 9(d), behaves similarly and is more negative than  $\gamma_{\text{approx}}$ . Although the magnitude of  $\gamma$  is not large, when it is integrated over times on the order of tens of milliseconds and exponentiated, the second factor in (39) becomes several orders of magnitude smaller than unity.

Combining the above ideas, we see that the effective range of integration in (39) may be regarded as the interval  $(x^2/\kappa, W - x/c)$ , where we have ignored dimensionless scale factors of the order unity. This interval shrinks to naught if

$$\frac{x^2}{\kappa} = W - \frac{x}{c}. \quad (44)$$

In other words, (44) identifies the edge of the zone where  $\delta\text{APD}(x)$  differs significantly from zero.

Let us show that (44) is satisfied approximately when

$$x \sim \varepsilon^{-1/6} \sqrt{\kappa\tau_{\text{out}}}. \quad (45)$$

First observe that from (41) that (45) comes from solving  $x^2/\kappa = W$ : i.e., neglecting the term  $x/c$  on the RHS of (44). This term may be neglected compared to  $W$  because, for the value of  $x$  given by (45), we see, after some rearranging of powers of the time constants and recalling (17), that

$$\frac{x}{c} \sim \varepsilon^{-1/6} \sqrt{\tau_{\text{in}}\tau_{\text{out}}} \sim \varepsilon^{1/6} \sqrt{\frac{\tau_{\text{in}}}{\tau_{\text{out}}}} W \ll W.$$

Thus, (45) estimates to leading order the width of the boundary-correction layer. Figure 10 shows that the  $\varepsilon^{-1/6}$  scaling for this width is quite accurate in the asymptotic range.

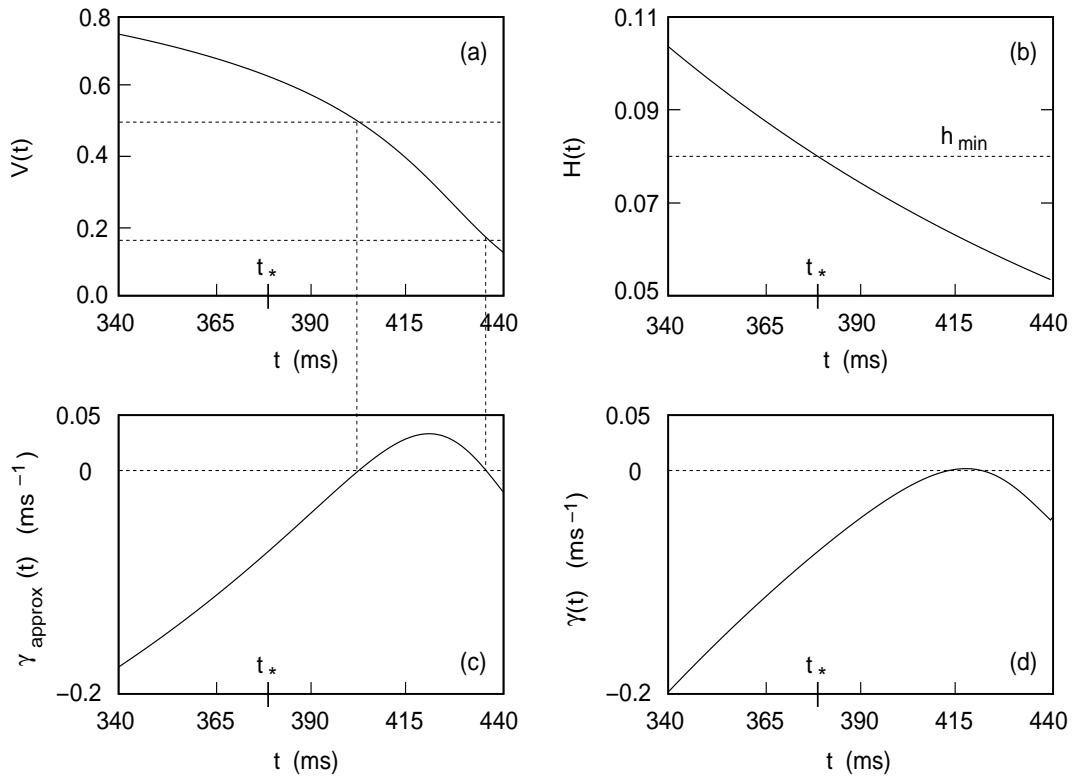


Figure 9: (a)  $V(t)$  versus  $t$ . Horizontal lines indicate  $V = 1/6$  and  $V = 1/2$ . (b)  $H(t)$  versus  $t$ . Note that  $h(t_*) = h_{\min}$ . (c)  $\gamma_{\text{approx}}$  versus  $t$ . Note that  $\gamma_{\text{approx}}$  vanishes when  $V$  passes through  $1/2$  and  $1/6$ . (d)  $\gamma$  versus  $t$ .

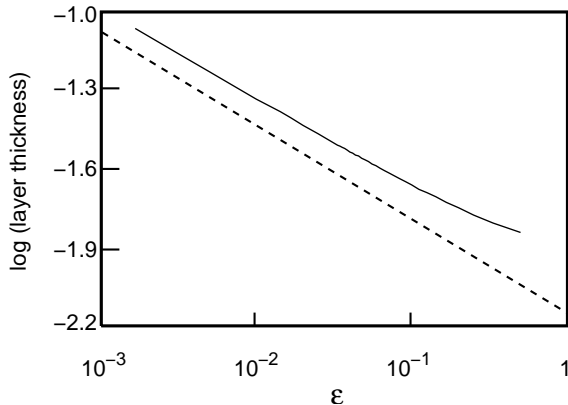


Figure 10: Log-log plot of layer thickness versus  $\varepsilon$ . Layer thickness was defined as the  $x$  value for which  $(\text{APD}_{\max} - \text{APD}(x))/(\text{APD}_{\max} - \text{APD}(0)) = 1/e$ . The dashed line has slope  $-1/6$  and is included for reference.

### 4.3 The approximation (27)

The approximation  $\gamma(x, t) \approx \gamma(0, t)$  is based on the fact that  $V(t + x/c), H(t + x/c)$ , the traveling-wave solution, does not vary greatly over the range of  $x$  where  $w$  differs significantly from zero. This range of  $x$  was estimated in (40). During repolarization, the derivative  $dV/d\xi$  is of the order at most  $\mathcal{O}(1/\tau_{\text{out}})$  while  $dH/d\xi$  is of the order  $\mathcal{O}(1/\tau_{\text{close}})$ . Thus, in the worst case

$$|V(t + x/c) - V(t)| \sim \frac{1}{\tau_{\text{out}}} \frac{\varepsilon^{-1/6} \sqrt{\kappa \tau_{\text{out}}}}{c} \sim \varepsilon^{-1/6} \sqrt{\frac{\tau_{\text{in}}}{\tau_{\text{out}}}}. \quad (46)$$

For the parameters in Table 1, the RHS of (46) is approximately 0.22, which is small but not extremely small. Thus, it is reassuring that, as illustrated in Figure 7, estimates based on the approximation (27) give highly accurate results.

### 4.4 Conclusions

In this paper we have studied how the duration of a propagating cardiac action potential is modified as it nears an insulating boundary. In order to obtain explicit analytical results, we described action potentials in a one-dimensional fiber using a simplified two-current model [8, 10]. Equation (39) estimates the shortening of APD at a site as a function of its distance from the boundary. As shown in Figure 7, this estimate agrees well with simulations. In (40) we determine how the width of the layer in which noticeable shortening occurs depends on the parameters in the model.

## Acknowledgments

Support of this research by the National Institutes of Health under grant 1R01-HL-72831 and the National Science Foundation under grant PHY-0549259 is gratefully acknowledged. We are also grateful to the referee, whose generous criticisms led to a much improved manuscript.

## References

- [1] M. BECK, C. JONES, D. SCHAEFFER, AND M. WECHSELBERGER, *Electrical waves in a one-dimensional model of cardiac tissue*, SIAM Appl. Dyn. Sys., submitted.
- [2] J. W. CAIN AND D. G. SCHAEFFER, *Two-term asymptotic approximation of a cardiac restitution curve*, SIAM Review, 48 (2006), pp. 537–546.
- [3] M. L. CARTWRIGHT, *Van der Pol's equation for relaxation oscillations*, in Contributions to the Theory of Nonlinear Oscillations, Vol. 2, S. Lefschetz, ed., Princeton University Press, Princeton, NJ, 1952, pp. 3–18.
- [4] H. DOBROVOLNY, *Spatial variation of cardiac restitution and the onset of alternans*, Ph.D. dissertation, Duke University, in preparation.
- [5] A. A. DORODNICYN, *Asymptotic solution of van der Pol's equation*, Prikladnaya Matematika i Mekhanika, 11 (1947), pp. 313–328 (in Russian); Amer. Math. Soc. Transl., 88 (1953) (English translation).
- [6] B. ECHEBARRIA AND A. KARMA, *Amplitude equation approach to spatiotemporal dynamics of cardiac alternans*, Phys. Rev. E, 76 (2007), pp. 051911.
- [7] J. J. FOX, M. L. RICCIO, F. HUA, E. BODENSCHATZ AND R. F. GILMOUR, JR., *Spatiotemporal transition to conduction block in canine ventricle*, Circ. Res., 90 (2002), pp. 289–296.
- [8] A. KARMA, *Spiral breakup in model equations of action potential propagation in cardiac tissue*, Phys. Rev. Lett., 71 (1993), pp. 1103–1107.
- [9] J. P. KEENER AND J. SNEYD, *Mathematical Physiology*, Springer-Verlag, New York, 1998.
- [10] C. C. MITCHELL AND D. G. SCHAEFFER, *A two-current model for the dynamics of cardiac membrane*, Bull. Math. Bio., 65 (2003), pp. 767–793.
- [11] J. D. MURRAY, *Mathematical Biology*, Springer-Verlag, New York, 1993.
- [12] A. M. PITRUZZELLO, W. KRASSOWSKA AND S. F. IDRIS, *Spatial heterogeneity of the restitution portrait in rabbit epicardium*, Amer. J. Physiol.: Heart and Circ. Physiol. 292 (2007), pp H1568–1578.

- [13] R. PLONSEY AND R. C. BARR, *Bioelectricity: A Quantitative Approach, 2nd Ed.*, Kluwer, New York, 2000.
- [14] W.A. STRAUSS, *Partial Differential Equations: An Introduction*, Wiley, New York, 1992.
- [15] YA. B. ZELDOVICH AND D.A. FRANK-KAMENETSKIĬ, *A theory of thermal flame propagation*, Zhurnal Fizicheskoi Khimii, 12 (1938), pp. 100–105. In Russian. English translation in, *Selected Works of Yakov Borisovich Zeldovich, Vol. 1*, Princeton University Press, Princeton, 1992.